IOP Publishing Journal of Physics D: Applied Physics
J. Phys. D: Appl. Phys. 40 (2007) 5588–5591 doi:10.1088/0022-3727/40/18/013

Temperature-dependent photoluminescence of undoped, N-doped and N-In codoped ZnO thin films

H B Ye[1], J F Kong[1], W Z Shen[1,3], J L Zhao[2] and X M Li[2]

[1] Laboratory of Condensed Matter Spectroscopy and Opto-Electronic Physics, Department of Physics, Shanghai Jiao Tong University, 1954 Hua Shan Road, Shanghai 200030, People's Republic of China
[2] State Key Laboratory of High Performance Ceramics and Superfine Microstructures, Shanghai Institute of Ceramics, Chinese Academy of Sciences, 1295 Ding Xi Road, Shanghai 200050, People's Republic of China

E-mail: wzshen@sjtu.edu.cn

Received 21 June 2007, in final form 3 August 2007
Published 30 August 2007
Online at stacks.iop.org/JPhysD/40/5588

Abstract
Temperature-dependent photoluminescence properties of undoped, N-doped and N-In codoped p-type ZnO thin films have been investigated in detail. The yielded temperature dependences of ultraviolet peak energy, width and intensity for several resolved emissions exhibit the different carrier recombination processes associated with doping mechanisms. We have revealed the acceptor binding energy of 113 meV, 140 meV and 112 meV and donor one of 56 meV, 82 meV and 112 meV for undoped, N-doped and N-In codoped ZnO, respectively, together with the broadening of the acceptor levels in N-doped and N-In codoped ZnO. We have also clarified the origin of the ZnO deep-level visible emission.

As a wide band gap (3.37 eV at room temperature) semiconductor with a large exciton binding energy (about 60 meV), ZnO has recently attracted much attention for optoelectronic devices, such as light-emitting diodes and laser diodes [1]. Due to the asymmetric doping limitations in ZnO [2], a great deal of effort has been made to realize the p-type doping of ZnO. Many groups have reported the fabrication of p-type ZnO by intentionally undoping [3], single-doping with Li [4], N [5, 6], P [7], As [8, 9] and Sb [10], as well as codoping techniques [11–13]. In contrast to the growth interest, the understanding of fundamental properties in p-type ZnO is still relatively incomplete, especially for the doping mechanisms and the acceptor and donor levels.

It is essential to understand the carrier recombination processes and the role of defects in p-type ZnO to fabricate the optoelectronic devices. Photoluminescence (PL) properties have been studied for p-ZnO of undoped [3] and single-doped with N [5], P [7], As [8] and Sb [10]. Recently, there is also a report on the compared PL study between P-doped and P-In codoped p-ZnO [13]. However, owing to the lack of effective methods to resolve the experimental emission spectra, the exact mechanisms of ultraviolet (UV) emission in ZnO and the corresponding carrier recombination processes are still subjects of considerable debates. Furthermore, compared with the interest in UV emission properties, the temperature-dependent behaviour of the visible emission in ZnO is rarely studied and the responsible defects remain controversial.

In this paper, we have presented a comprehensive investigation of temperature-dependent PL properties of undoped, N-doped and N-In codoped p-type ZnO thin films grown by ultrasonic spray pyrolysis (USP). Through multi-Gaussian fittings to the experimental spectra, the temperature dependences of UV peak energy, width and intensity have been obtained and fitted to reveal the different carrier recombination processes and doping mechanisms. In addition, the mechanism of the deep-level visible emission in ZnO has also been discussed.

The studied undoped, N-doped and N-In codoped ZnO thin films were deposited by USP at atmosphere [11]. The $Zn(CH_3COO)_2 \cdot 2H_2O$ (AR, 0.5 mol l^{-1}), CH_3COONH_4(AR, 2.5 mol l^{-1}) and $In(NO_3)_3$ (AR, 0.5 mol l^{-1}) were chosen as the sources of Zn, N and In, respectively. The atomic

[3] Author to whom any correspondence should be addressed.

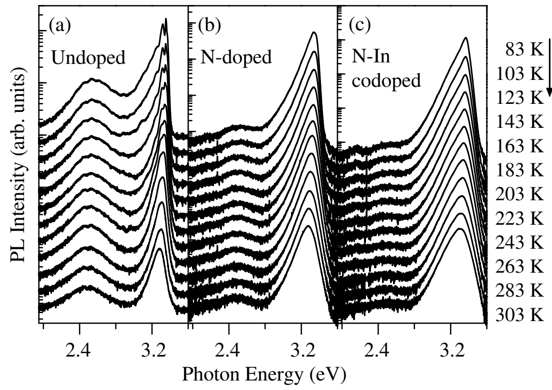

Figure 1. Temperature-dependent PL spectra of (*a*) undoped, (*b*) N-doped and (*c*) N-In codoped ZnO measured from 83 to 303 K. The intensity is shown on a logarithmic scale.

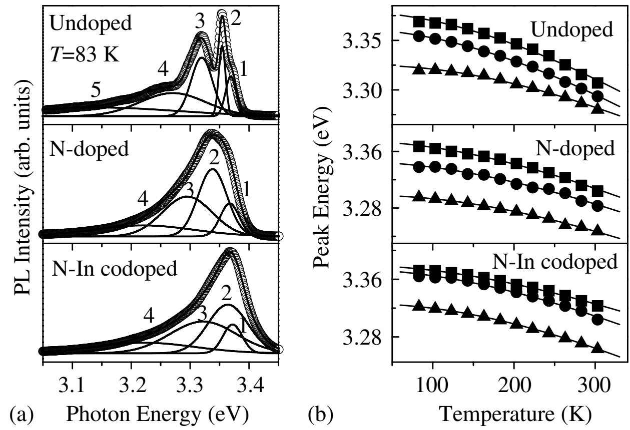

Figure 2. (*a*) NBE PL spectra at 83 K for undoped, N-doped and N-In codoped ZnO, where the solid curves show the Gaussian deconvolution of the experimental spectra (○). (*b*) Temperature-dependent peak energies and the fitting curves for bands 1 (■), 2 (●) and 3 (▲) in (*a*). Bands 1, 2 and 3 are assigned to FX, A^0X and eA^0, respectively.

ratio of Zn/N was 1 : 3 for the N-doped film, and Zn/N/In was 1 : 3 : 0.05 for the N-In codoped film. The intrinsic Si (1 0 0) wafers (conductivity of $10^{-4}\ \Omega^{-1}\ \mathrm{cm}^{-1}$) were used as the substrates, which were heated to 450 °C. All films were controlled to be 300 nm thick. Room-temperature Hall measurements were taken in the Van der Pauw configuration at the magnetic field of 0.5 T, showing the p-type conductivity of $1.14\ \Omega^{-1}\ \mathrm{cm}^{-1}$, $1.51\ \Omega^{-1}\ \mathrm{cm}^{-1}$ and $2.01\ \Omega^{-1}\ \mathrm{cm}^{-1}$, hole density p of $6.60 \times 10^{16}\ \mathrm{cm}^{-3}$, $1.26 \times 10^{17}\ \mathrm{cm}^{-3}$ and $2.46 \times 10^{17}\ \mathrm{cm}^{-3}$ and hole mobility μ_p of $108\ \mathrm{cm}^2\ \mathrm{V}^{-1}\ \mathrm{s}^{-1}$, $75\ \mathrm{cm}^2\ \mathrm{V}^{-1}\ \mathrm{s}^{-1}$ and $51\ \mathrm{cm}^2\ \mathrm{V}^{-1}\ \mathrm{s}^{-1}$ for undoped, N-doped and N-In codoped ZnO, respectively. We have demonstrated the good agreement of p and μ_p between room-temperature Raman and Hall measurements in N-In codoped ZnO [14], while the effective N-In codoping and high hole mobility have also been confirmed in our previous work [15]. Temperature-dependent PL measurements from 83 to 303 K were carried out on a Jobin Yvon LabRAM HR 800UV micro-Raman system with an Andor DU420 classic CCD detector and a Linkam THMS600 temperature stage under the excitation of a He–Cd laser (325 nm).

Figures 1(*a*)–(*c*) show the experimental PL spectra of undoped, N-doped and N-In codoped ZnO measured from 83 to 303 K. Note that the intensity is displayed on a logarithmic scale. Generally, the PL spectrum of ZnO consists mainly of a near band edge (NBE) emission in the UV region and a deep-level emission in the visible region due to structural defects and impurities [1]. As shown in figure 1(*a*), the spectra of undoped ZnO clearly exhibit several resolved NBE emissions at low temperatures with a broad visible emission centred at about 2.5 eV. For the spectra of N-doped (figure 1(*b*)) and N-In codoped ZnO (figure 1(*c*)), an asymmetrical and combinational NBE emission is observed and becomes broader and broader compared with the undoped one, while the visible emissions become much weaker in N-doped film and are almost undetectable in codoped film. All the above luminescence behaviours indicate different carrier recombination processes associated with doping mechanisms.

To better understand the nature of the NBE emission and different carrier recombination processes, we have performed the multi-Gaussian fittings to the experimental spectra throughout the measured temperature range. Figure 2(*a*) illustrates 83 K PL spectra (open circles) of undoped, N-doped and N-In codoped ZnO with the multi-Gaussian fitting results (solid curves). Here, we use the least Gaussian bands to fit the PL spectra and the obtained self-consistent results testify to the reliability of the method. The best fitting result for undoped ZnO consists of five bands labelled as 1, 2, 3, 4 and 5, respectively. For N-doped and N-In codoped ZnO, the spectra are resolved into four individual bands labelled as 1, 2, 3 and 4, respectively. According to [3, 13], the resolved excitonic features in p-type ZnO are unlikely to be observed clearly from the PL spectra even at temperatures much lower than 83 K. The obtained temperature-dependent peak energies $E(T)$ of bands 1 (squares), 2 (circles) and 3 (triangles) for the three samples are displayed in figure 2(*b*). It can be observed that bands 1 and 2 systematically shift to lower energy with increasing temperature and their energy shifts can be well described by the Varshni equation $E(T) = E(0) - \alpha T^2/(T+\beta)$ [16], where $E(0)$ is the transition energy at 0 K, α is related to the exciton-average phonon interaction and β is closely related to the Debye temperature. The energy shift of band 3 can be expressed as the Varshni equation plus $k_B T/2$, where k_B is the Boltzmann constant. The solid curves in figure 2(*b*) are least-squares fits with the fitting parameters summarized in table 1 (we assumed $\beta = 920$ K according to [17]). The yielded α is close to the reported values [18]. For clearness, we have also listed the differences between $E_g(0)$ and $E(0)$ in table 1, where $E_g(0) = 3.437$ eV is the ZnO band gap at 0 K.

From the above analysis, we can assign the band 1 to free exciton (FX) emission and its binding energy is 58 meV, 62 meV and 58 meV for undoped, N-doped and N-In codoped ZnO, respectively. Band 2 corresponds to neutral-acceptor-bound exciton (A^0X) emission and the band 3 is assigned to free-electron-to-neutral-acceptor transition (eA^0). As the transition energy of eA^0 can be written as $E_{eA} = E_g - E_A + k_B T/2$ [8], the obtained acceptor binding energy E_A is 113 meV, 140 meV and 112 meV for undoped, N-doped and N-In codoped ZnO, respectively. The emissions of band 4 at 3.271, 3.220 and 3.222 eV for the three samples shown in figure 2(*a*) should correspond to the donor–acceptor pair (DAP) transition. In this case, the donor

Table 1. Results of fitting peak energy and width for bands 1 (FX), 2 (A^0X) and 3 (eA^0) in undoped, N-doped and N-In codoped ZnO. Here $E_g(0) = 3.437$ eV.

Sample	Band	$E(0)$ (eV)	α (10^{-4} eV K^{-1})	$E_g(0) - E(0)$ (meV)	Γ_0 (meV)	γ_{ph} (meV K^{-1})	Γ_{LO} (meV)
Undoped ZnO	1	3.379	9.20	58	16	0.033	435
	2	3.361	8.96	76	11	0.017	594
	3	3.324	7.38	113	35	0.022	690
N-doped ZnO	1	3.375	9.09	62	25	0.101	502
	2	3.346	8.12	91	36	0.171	61
	3	3.297	8.55	140	74	0.128	339
N-In codoped ZnO	1	3.379	7.28	58	28	0.066	539
	2	3.373	8.75	64	42	0.287	171
	3	3.325	10.00	112	98	0.212	267

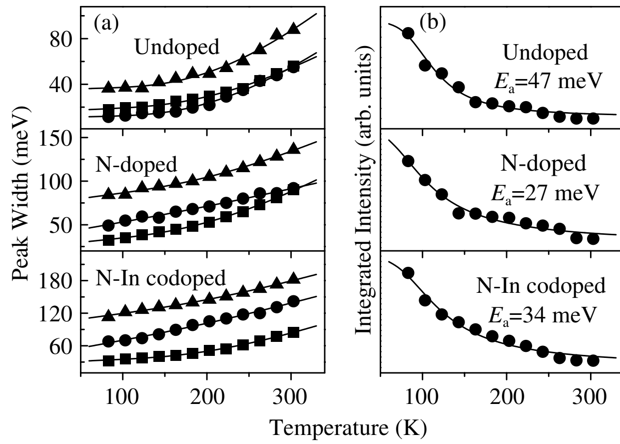

Figure 3. (*a*) Temperature-dependent peak widths and the fitting curves for bands 1 (■), 2 (●) and 3 (▲) in undoped, N-doped and N-In codoped ZnO. (*b*) Integrated PL intensity and the fitting curves for the band 2 (●) as a function of temperature. Bands 1, 2 and 3 are assigned to FX, A^0X and eA^0, respectively.

binding energy E_D can be estimated from the equation $E_D = E_g - E_A - E_{DAP} + \sqrt[3]{4\pi/3}(e^2/4\pi\varepsilon\varepsilon_0)N_{A,D}^{1/3}$ [6], where $N_{A,D}$ is the majority impurity concentration, $\varepsilon = 8.656$ is the specific dielectric constant and ε_0 is the dielectric constant in a vacuum. Making $N_{A,D}$ approximately equal to the hole density, we have E_D of 56 meV, 82 meV and 112 meV for undoped, N-doped and N-In codoped ZnO, respectively. In addition, the weak emission of band 5 at 3.143 eV in undoped ZnO is attributed to the zinc vacancy (V_{Zn})-related defect [3]. Although the nature of shallow acceptor is difficult to identify in undoped ZnO, the obtained E_D of 56 meV is in good agreement with the reported 56–58 meV [19]. E_A of 140 meV in N-doped film corresponds to N_O acceptor while the smaller E_A of 112 meV in N-In codoped ZnO is attributed to $2N_O$–In_{Zn} acceptor complex, which complies with the theoretical prediction of reduced acceptor transition energy due to the codoping technique [20]. On the other hand, the N-doping and N-In codoping in ZnO result in the deeper and deeper donor level according to E_D. Thus fewer and fewer free electrons can be activated to compensate holes. The enhanced hole density from Hall measurements in N-doped and N-In codoped ZnO is the best demonstration.

Figure 3(*a*) displays the temperature dependence of peak width $\Gamma(T)$ of bands 1 (squares), 2 (circles) and 3 (triangles) for undoped, N-doped and N-In codoped ZnO. The smaller peak width of bands 1 and 2 (FX and A^0X) than that of band 3 (eA^0) is due to the excitonic properties, which further supports the above assignments. The solid curves are least-square fits using the equation $\Gamma(T) = \Gamma_0 + \gamma_{ph}T + \Gamma_{LO}/[\exp(\hbar\omega_{LO}/k_BT) - 1]$ [21], where $\hbar\omega_{LO} = 72$ meV is the energy of a longitudinal optical (LO) phonon, Γ_0 is the intrinsic line width at 0 K, γ_{ph} is the exciton-acoustic phonon coupling constant and Γ_{LO} represents the exciton-LO phonon (Fröhlich) coupling strength. The fitting parameters are also listed in table 1. Among them, the values of Γ_{LO} are much larger than those of γ_{ph}, which is mainly owing to the high Fröhlich constant and the LO energy. For the values of Γ_0, the ratios between N-doped and undoped ZnO are 1.56, 3.27 and 2.11 for FX, A^0X and eA^0, respectively, while the corresponding ratios are 1.75, 3.82 and 2.80 in codoped film. This broadening behaviour is attributed to the doping mechanisms. With the enhanced hole density by N-doping and N-In codoping, more temperature-independent mechanisms including hole–hole interaction and impurity will be introduced to broaden Γ_0. On the other hand, the N-doping and N-In codoping will broaden the acceptor level in the band gap [20], which directly leads to the stronger broadening of A^0X and eA^0 emissions than FX.

Figure 3(*b*) shows the integrated intensity of A^0X (band 2) emission as a function of temperature for the three samples. The observed overall temperature-quenching behaviour can be well described by the equation $I(T) = I_0/[1 + A\exp(-E_a/k_BT)]$ [22], where I_0 is the emission intensity at zero temperature, A is a parameter and E_a is the activation energy in the thermal quenching process. The good fits (solid curves) yielded E_a of 47 meV, 27 meV and 34 meV for undoped, N-doped and N-In codoped ZnO, respectively. In order to understand the thermal quenching process, the localization energy E_{loc} (FX-A^0X) of 18 meV, 29 meV and 6 meV for undoped, N-doped and N-In codoped ZnO, respectively, has been obtained to compare with E_a. We identify the dissociation process of A^0X to a FX and a neutral acceptor in N-doped ZnO because of the comparable values of the activation and localization energy. For undoped and codoped ZnO, the difference between E_a and E_{loc} is 29 and 28 meV. Considering the corresponding E_A of 113 and 112 meV, we can deduce almost the same Haynes factor of 0.25. Therefore, the quenching processes include the thermal ionization of acceptor besides the above dissociation in undoped and N-In codoped films.

The reported visible emission in ZnO was attributed to different types of electron transitions in various defects involving oxygen vacancy (V_O), V_{Zn}, zinc interstitial (Zn_i)

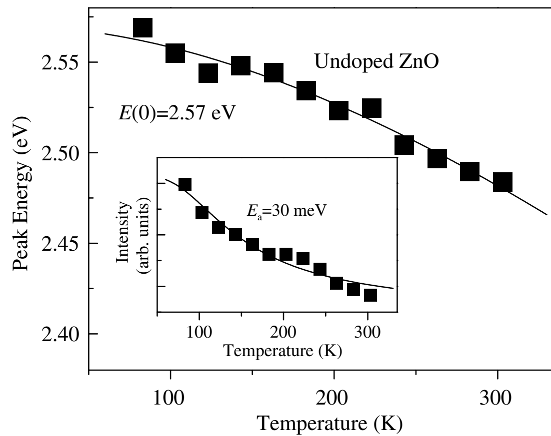

Figure 4. Temperature dependence of deep-level emission energy in undoped ZnO. The inset shows the integrated intensity as a function of temperature. The solid curves are the fitting results.

and O_{Zn} [1]. To clarify its origin, we have calculated the temperature-dependent peak energies of the deep-level emission in undoped ZnO (figure 4) from the good single-Gaussian fittings of the experimental spectra. Since the deep-level emission follows the shrinkage of the band gap with increasing temperature (solid curve by Varshni fitting), we exclude the possibility of the transition within localized defects. The obtained $E(0)$ of 2.57 eV clearly indicates that this deep-level emission is caused by the electron transition from the V_O donor level to the valence band [23]. The inset of figure 4 presents the corresponding integrated intensity as a function of temperature. The yielded E_a through fitting to the thermal quenching equation (solid curve) is 30 meV, which is close to the reported value [24] and may attribute to the process $V_O^x \rightarrow V_O^\bullet + e$. Furthermore, as interpreted above, fewer and fewer free electrons can be thermally activated in N-doped and N-In codoped ZnO, i.e. weaker and weaker deep-level emissions in figure 1, confirming again the electron transition for the ZnO deep-level emission.

In summary, we have performed the multi-Gaussian fittings to the experimental NBE spectra of undoped, N-doped and N-In codoped p-type ZnO in the temperature range from 83 to 303 K. With the assignments of FX, A^0X and eA^0 transitions, the temperature dependences of UV peak energy, width and intensity have been analysed in detail. The obtained E_A of 113 meV, 140 meV and 112 meV with E_D of 56 meV, 82 meV and 112 meV for undoped, N-doped and N-In codoped ZnO, respectively, exhibits good correlations with the different carrier recombination processes. The broadening of acceptor levels has been observed in N-doped and N-In codoped ZnO. In addition, we have confirmed that the deep-level visible emission in ZnO originates from the electron transition from the V_O donor level to the valance band.

Acknowledgments

This work was supported by the Natural Science Foundation of China (contract Nos 10674094, 60576067 and 90401010), National Major Basic Research Project of 2006CB921507, the Minister of Education of PCSIRT (contract No IRT0524), and the Shanghai Municipal Commission of Science and Technology Projects of 05QMH1411 and 06JC14039.

References

[1] Özgür Ü, Alivov Ya I, Liu C, Teke A, Reshchikov M A, Doğan S, Avrutin V, Cho S-J and Morkoc H 2005 *J. Appl. Phys.* **98** 041301
[2] Yamamoto T and Yoshida H K 2001 *Physica* B **302–303** 155
[3] Zeng Y J, Ye Z Z, Xu W Z, Lu J G, He H P, Zhu L P, Zhao B H, Che Y and Zhang S B 2006 *Appl. Phys. Lett.* **88** 262103
[4] Zeng Y J, Ye Z Z, Xu W Z, Li D Y, Lu J G, Zhu L P and Zhao B H 2006 *Appl. Phys. Lett.* **88** 062107
[5] Wang L and Giles N C 2004 *Appl. Phys. Lett.* **84** 3049
[6] Look D C, Reynolds D C, Litton C W, Jones R L, Eason D B and Cantwell G 2002 *Appl. Phys. Lett.* **81** 1830
[7] Xiu F X, Yang Z, Mandalapu L J, Liu J L and Beyermann W P 2006 *Appl. Phys. Lett.* **88** 052106
[8] Ryu Y R, Lee T S and White H W 2003 *Appl. Phys. Lett.* **83** 87
[9] Look D C, Renlund G M, Burgener R H II and Sizelove J R 2004 *Appl. Phys. Lett.* **85** 5269
[10] Xiu F X, Yang Z, Mandalapu L J, Zhao D T and Liu J L 2005 *Appl. Phys. Lett.* **87** 252102
[11] Bian J M, Li X M, Gao X D, Yu W D and Chen L D 2004 *Appl. Phys. Lett.* **84** 541
[12] Lu J G, Ye Z Z, Zhuge F, Zeng Y J, Zhao B H and Zhu L P 2004 *Appl. Phys. Lett.* **85** 3134
[13] Ye J D, Gu S L, Li F, Zhu S M, Zhang R, Shi Y, Zheng Y D, Sun X W, Lo G Q and Kwong D L 2007 *Appl. Phys. Lett.* **90** 152108
[14] Kong J F, Chen H, Ye H B, Shen W Z, Zhao J L and Li X M 2007 *Appl. Phys. Lett.* **90** 041907
[15] Ye H B, Kong J F, Shen W Z, Zhao J L and Li X M 2007 *Appl. Phys. Lett.* **90** 102115
[16] Varshni Y P 1967 *Physica* **34** 149
[17] Hutson A R 1959 *J. Phys. Chem. Solids* **8** 467
[18] Ko H J, Chen Y F, Zhu Z, Yao T, Kobayashi I and Uchiki H 2000 *Appl. Phys. Lett.* **76** 1905
[19] Reynolds D C, Look D C, Jogai B, Litton C W, Collins T C, Harsch W C and Cantwell G 1998 *Phys. Rev.* B **57** 12151
[20] Yamamoto T 2003 *Japan. J. Appl. Phys.* Part 2 **42** L514
[21] Makino T, Chia C H, Tuan N T, Segawa Y, Kawasaki M, Ohtomo A, Tamura K and Koinuma H 2000 *Appl. Phys. Lett.* **76** 3549
[22] Shen W Z and Shen S C 1996 *J. Appl. Phys.* **80** 5941
[23] Kang H S, Kang J S, Kim J W and Lee S Y 2004 *J. Appl. Phys.* **95** 1246
[24] Liu Z S, Jing X P, Wang L X and Li Y 2006 *J. Electrochem. Soc.* **153** G1035